PAPER

Channel Prediction Techniques for a Multi-User MIMO System in Time-Varying Environments

Kanako YAMAGUCHI[†], ***Student Member***, **Huu Phu BUI**[††*], ***Nonmember***, **Yasutaka OGAWA**[†a)], ***Fellow***, **Toshihiko NISHIMURA**[†], ***and*** **Takeo OHGANE**[†], ***Members***

SUMMARY Although multi-user multiple-input multiple-output (MIMO) systems provide high data rate transmission, they may suffer from interference. Block diagonalization and eigenbeam-space division multiplexing (E-SDM) can suppress interference. The transmitter needs to determine beamforming weights from channel state information (CSI) to use these techniques. However, MIMO channels change in time-varying environments during the time intervals between when transmission parameters are determined and actual MIMO transmission occurs. The outdated CSI causes interference and seriously degrades the quality of transmission. Channel prediction schemes have been developed to mitigate the effects of outdated CSI. We evaluated the accuracy of prediction of autoregressive (AR)-model-based prediction and Lagrange extrapolation in the presence of channel estimation error. We found that Lagrange extrapolation was easy to implement and that it provided performance comparable to that obtained with the AR-model-based technique.

key words: *channel prediction, multi-user MIMO system, block diagonalization, eigenbeam-space division multiplexing, time-varying environments, AR model, lagrange extrapolation*

1. Introduction

Multi-user multiple-input multiple-output (MIMO) systems have been widely studied because they provide high data rate transmission [1], [2]. A base station (BS) in a downlink transmission senario simultaneously sends signals to multiple users. Thus, we may encounter inter-user interference (IUI) that can seriously degrade performance. A block diagonalization (BD) scheme [3], [4] can be applied to eliminate IUI. This scheme block-diagonalizes multi-user MIMO channels, and forces interference to other users to reach zero. Although IUI can be suppressed by using the BD scheme, inter-stream interference (IStI) occurs because the BS may transmit multiple streams to each mobile station (MS). We can suppress IStI by using eigenbeam-space division multiplexing (E-SDM) [5] that partitions MIMO channels into orthogonal channels by forming eigenbeams. The transmitter needs to determine beamforming weights from channel state information (CSI) for these techniques to be used.

Propagation environments in wireless communication systems vary over time. MIMO channels change during the time intervals between when transmission parameters are determined and actual MIMO transmission occurs in time-varying environments, where the transmission weights are no longer optimum [6]. Hence, performance is seriously degraded because we cannot suppress interference by using the outdated beamforming weights. Channel prediction techniques [7]–[12] can be used to mitigate the effect of outdated CSI. One typical scheme is a linear predictor based on the autoregressive (AR) model [13]. The predictor needs the AR coefficients determined from the Yule-Walker equation to predict future channels. The autocorrelations of the channels are needed to obtain the Yule-Walker equation. Since many data points are required, channel autocorrelations are not easy to estimate accurately in actual environments. Thus far, we have calculated autocorrelations assuming the Jakes' model [14], [15]. However, even in this case, we need the maximum Doppler frequency to obtain the autocorrelations. It is not necessarily easy to accurately estimate values for the maximum Doppler frequency in actual environments. In contrast, the Lagrange extrapolation scheme [16], [17] can predict future channels without parameters such as autocorrelations or maximum Doppler frequency. This method can predict future channels with simple extrapolation using past channels alone. As a result, we can easily implement the Lagrange scheme.

Reference [6] describes the channel prediction effect for the multi-user MIMO system. The evaluations were, however, limited to a linear extrapolation in the Lagrange extrapolation. The prediction performance degrades depending on time-varying situations. Also, ideal channel estimation was assumed and channel estimation error due to receiver noise was not taken into account. Based on the previous work, we examined what effects AR-model-based prediction and Lagrange extrapolation (linear, second-order, and third-order extrapolations) had on multi-user MIMO downlink transmission. We evaluated performance in cases of the Jakes' model and an actual indoor environment. MIMO channels were estimated using finite pilot symbols, and the evaluations were done in the presence of channel estimation error.

The paper is organized as follows. The next section

Manuscript received March 27, 2014.
Manuscript revised July 24, 2014.

[†]The authors are with the Graduate School of Information Science and Technology, Hokkaido University, Sapporo-shi, 060-0814 Japan.

[††]The author is with the National Key Lab of Digital Control & System Engineering, University of Technology, Vietnam National University, Hochiminh City, Vietnam.

[*]The work of H. P. Bui was supported in part by National Key Laboratory of Digital Control and System Engineering (DCSE-LAB), University of Technology, Vietnam National University - Hochiminh City.

a) E-mail: ogawa@ist.hokudai.ac.jp

DOI: 10.1587/transcom.E97.B.2747

briefly describes the multi-user MIMO system and channel prediction methods. We evaluated performance in different time-varying environments, which is discussed in Sect. 3. Finally, Sect. 4 provides our conclusions.

2. Multi-User MIMO System and Channel Prediction

Let us consider a downlink multi-user MIMO system based on a combination of the BD scheme and the E-SDM technique to suppress IUI and IStI. General and detailed descriptions of the BD scheme and the E-SDM technique have been given in Spencer et al. [3] and Miyashita et al. [5]. A BS in this system with N_T antennas simultaneously transmits signals to K users (mobile stations (MSs)), and each MS has N_R antennas. The BS needs CSI to determine the transmit (TX) weights to use these techniques. Here, we have assumed packet transmission [2] in the time division duplexing (TDD) system shown in Fig. 1. Uplink and downlink signals are transmitted with a period of the frame duration, T_f. The BS estimates the channels for the MSs using uplink acknowledge (ACK) packets, and determines the TX weights based on the BD scheme and the E-SDM technique.

As stated in the literature [6], the TX weights suppress IUI and IStI for the channels. We express the channel matrix and the TX weight matrix for the kth MS at time t as $\boldsymbol{H}_k(t)$ and $\boldsymbol{W}_{\mathrm{TX},k}(t)$, respectively. Since the TX weight matrices are determined with the BD scheme, the IUI is suppressed and we have

$$\boldsymbol{H}_m(t)\boldsymbol{W}_{\mathrm{TX},k}(t) = \begin{cases} \tilde{\boldsymbol{H}}_k(t) & (m = k) \\ 0 & (m \neq k) \end{cases}. \tag{1}$$

Here, the elements in $\tilde{\boldsymbol{H}}_k(t)$ are referred to as effective downlink channels including the effects of the TX weights. We assume that channel changes during the ACK packets are negligibly small and do not affect the channel estimation. The BS, however, sends downlink packets with delay τ from the ACK packets. The channels change during the delay in time-varying environments where MSs and/or surrounding scatterers move, and we have

$$\boldsymbol{H}_m(t+\tau) = \boldsymbol{H}_m(t) + \Delta\boldsymbol{H}_m(t,\tau). \tag{2}$$

The TX weight matrices $\boldsymbol{W}_{\mathrm{TX},k}(t)$ are outdated for the downlink multi-user transmission. Then, instead of (1), we have

$$\begin{aligned} &\boldsymbol{H}_m(t+\tau)\boldsymbol{W}_{\mathrm{TX},k}(t) \\ &= \{\boldsymbol{H}_m(t) + \Delta\boldsymbol{H}_m(t,\tau)\}\,\boldsymbol{W}_{\mathrm{TX},k}(t) \\ &= \begin{cases} \tilde{\boldsymbol{H}}'_k(t,\tau) & (m = k) \\ \Delta\boldsymbol{H}_m(t,\tau)\boldsymbol{W}_{\mathrm{TX},k}(t) & (m \neq k) \end{cases}, \end{aligned} \tag{3}$$

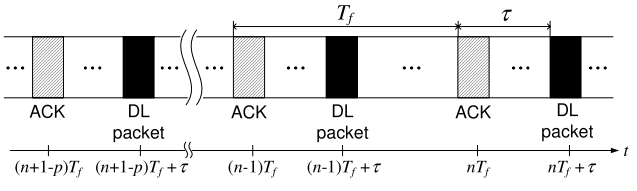

Fig. 1 TDD transmission frame format.

where

$$\tilde{\boldsymbol{H}}'_k(t,\tau) = \tilde{\boldsymbol{H}}_k(t) + \Delta\boldsymbol{H}_k(t,\tau)\boldsymbol{W}_{\mathrm{TX},k}(t). \tag{4}$$

As seen from the above equation, the outdated TX weights cause the IUI, $\Delta\boldsymbol{H}_m(t,\tau)\boldsymbol{W}_{\mathrm{TX},k}(t)$ for $m \neq k$. Since $\tilde{\boldsymbol{H}}_k^H(t)\tilde{\boldsymbol{H}}_k(t)$ is a diagonal matrix, maximal ratio combining at MSs does not cause IStI. The effective downlink channels are, however, not $\tilde{\boldsymbol{H}}_k(t)$ but are $\tilde{\boldsymbol{H}}'_k(t,\tau)$ due to the delay τ. Since $\tilde{\boldsymbol{H}}'^H_k(t,\tau)\tilde{\boldsymbol{H}}'_k(t,\tau)$ is not a diagonal matrix, MSs suffer from IStI if we employ the maximal ratio combining. Even when the channel estimation is carried out accurately using the ACK packets, the interference is caused in the time-varying channels and the performance of multi-user transmission is deteriorated. If we can predict future channels when data are transmitted by using past channels, IUI and IStI can be decreased. We will briefly describe channel prediction schemes below.

2.1 Channel Prediction Based on AR Model

We represent the channel from the jth TX antenna of the BS to the ith receive (RX) antenna of the kth MS at time t by $h_{ij,k}(t)$. The future channel at downlink packet transmission time, $nT_f + \tau$, predicted by the AR-model-based algorithm is given by

$$\hat{h}^A_{ij,k}\left(nT_f + \tau\right) = \sum_{m=1}^{p} a_m h_{ij,k}\left((n+1-m)\,T_f\right). \tag{5}$$

Here, a_m are AR coefficients, and p is called the AR model order. The optimum AR coefficients are determined by using the Yule-Walker equation

$$\boldsymbol{R}\boldsymbol{a} = \boldsymbol{r}'. \tag{6}$$

The $\boldsymbol{a}$ is the p-dimensional vector in Eq. (6) defined as

$$\boldsymbol{a} = \left[a_1,\ a_2,\ \cdots,\ a_p\right]^T, \tag{7}$$

where $[\cdot]^T$ denotes the transpose. The $\boldsymbol{R}$ is the $p \times p$ correlation matrix whose l_1th row and l_2th column elements are given by

$$\begin{aligned} r\,(l_1 - l_2) &= r^*\,(l_2 - l_1) \\ &= E\left\{h^*_{ij,k}\left((n+1-l_1)\,T_f\right)h_{ij,k}\left((n+1-l_2)\,T_f\right)\right\} \\ &= E\left\{h^*_{ij,k}\left((n-(l_1-l_2))\,T_f\right)h_{ij,k}\left(nT_f\right)\right\}, \end{aligned} \tag{8}$$

where * denotes the complex conjugate and $E\{\cdot\}$ denotes the ensemble average. Also, the lth element of the pth dimensional correlation vector, $\boldsymbol{r}'$, is given by

$$r'(l) = E\left\{h^*_{ij,k}\left((n+1-l)\,T_f\right)h_{ij,k}\left(nT_f + \tau\right)\right\}. \tag{9}$$

We need the autocorrelations of channels to solve Eq. (6). However, it is not easy to accurately estimate autocorrelations in actual environments. We obtained autocorrelations assuming the Jakes' model, and the autocorrelation function

is given by

$$E\left\{h^*_{ij,k}(t-T)\,h_{ij,k}(t)\right\} = J_0(2\pi f_D T), \tag{10}$$

where $J_0(\cdot)$ is the Bessel function of the first kind of order zero and f_D is the maximum Doppler frequency. Note that we ignore the constant coefficient in Eq. (10), which does not affect the AR coefficients. Thus, Eqs. (8) and (9) are rewritten as

$$\begin{aligned} r(l_1 - l_2) &= r(l_2 - l_1) \\ &= J_0\left(2\pi f_D (l_1 - l_2) T_f\right) \end{aligned} \tag{11}$$

$$r'(l) = J_0\left(2\pi f_D\left(\tau + (l-1)T_f\right)\right). \tag{12}$$

Substituting Eqs. (11) and (12) into Eq. (6), we can obtain the AR coefficients and compute future channels.

2.2 Lagrange Extrapolation

We presented AR-model-based prediction in the previous subsection that assumed the Jakes' model. Even in this case, we need the maximum Doppler frequency, f_D, to obtain the autocorrelations. However, it is not necessarily easy to accurately estimate values in actual environments.

Lagrange extrapolation, on the other hand, is extremely easy to implement. The method does not need either channel autocorrelations or the maximum Doppler frequency. We evaluated linear, second-order, and third-order extrapolations of the Lagrange extrapolation schemes.

A future channel is linearly extrapolated in linear extrapolation with the last two channels and is given by

$$\begin{aligned} &\hat{h}^L_{ij,k}\left(nT_f + \tau\right) \\ &= h_{ij,k}\left(nT_f\right) + \frac{\tau}{T_f}\left(h_{ij,k}\left(nT_f\right) - h_{ij,k}\left((n-1)T_f\right)\right). \end{aligned} \tag{13}$$

The values predicted by the quadratic function using the last three channels and the cubic function using the last four channels are similarly respectively given by Eqs. (14) and (15). They correspond to second-order and third-order extrapolations.

We can estimate channels by using past channels alone as can be seen from Eqs. (13)–(15). As a result, the Lagrange scheme is much easier than AR-based extrapolation with respect to implementation.

3. Analyses of Performance in Channel Predictions

We examined the prediction effects for multi-user MIMO downlink channels in cases of the correlated and uncorrelated Jakes' model and an actual indoor environment. We conducted simulations of a multi-user MIMO E-SDM system by assuming the parameters listed in Table 1. We assumed that the data rate for each MS was fixed constantly at 4 bps/Hz (4 bits per symbol duration). Because the TX had four antennas and each RX had two antennas, we had either single-stream (16 QAM: quadrature amplitude modulation) or two-stream (2 × QPSK: quaternary phase shift keying) transmission for each RX. Determining the number of streams, modulation scheme, and TX power was done in such a way that the Chernoff upper bound of the bit error rate (BER) for each MS had the lowest value [5]. The total TX power per MS was the same. We assumed frequency-flat fading channels. The uplink channels were estimated at the TX using pilot symbols in the ACK packets, and the effective downlink channels ($\tilde{\boldsymbol{H}}'_k(t,\tau)$) for E-SDM transmission were estimated at both RXs using pilot symbols in the downlink packets. For each uplink channel, N_p pilot symbols in each ACK packet were used for estimation. For each effective downlink channel, N_p pilot symbols multiplied by the transmit weights in each downlink packet were sent for estimation. Because all the pilot symbols were 1 in the simulations, each channel was obtained by averaging the N_p pilot symbols. The effective SNR for channel estimation is N_p times higher than a single pilot symbol case. All the pilot

Table 1 Simulation parameters.

No. of MSs	2
No. TX & RX antennas	4 × 2
Data rate for each MS	4 bits/symbol/user
Modulation schemes	QPSK, 16QAM
Resource control	Minimum BER criterion based on Chernoff upper bound [5]
Data burst length in a downkink packet	128 symbols
Frame duration (T_f)	10 ms
Center frequency (f_c)	5.275 GHz
Max. Doppler frequency (f_D)	18.6 Hz
Thermal noise	Additive white Gaussian noise
RX signal processing	MMSE weight

$$\begin{aligned} \hat{h}^S_{ij,k}\left(nT_f + \tau\right) =& h_{ij,k}\left((n-2)T_f\right) + \frac{\left(2T_f + \tau\right)}{T_f}\left(h_{ij,k}\left((n-1)T_f\right) - h_{ij,k}\left((n-2)T_f\right)\right) \\ &+ \frac{\left(2T_f + \tau\right)\left(T_f + \tau\right)}{2T_f^2}\left(h_{ij,k}\left(nT_f\right) - 2h_{ij,k}\left((n-1)T_f\right) + h_{ij,k}\left((n-2)T_f\right)\right) \end{aligned} \tag{14}$$

$$\begin{aligned} \hat{h}^T_{ij,k}\left(nT_f + \tau\right) =& h_{ij,k}\left(nT_f\right) - \frac{\left(2T_f + \tau\right)\left(T_f + \tau\right)\tau}{6T_f^3}\left(h_{ij,k}\left((n-3)T_f\right) - 3h_{ij,k}\left((n-2)T_f\right) + 3h_{ij,k}\left((n-1)T_f\right) - h_{ij,k}\left(nT_f\right)\right) \\ &+ \frac{\left(T_f + \tau\right)\tau}{2T_f^2}\left(h_{ij,k}\left((n-2)T_f\right) - 2h_{ij,k}\left((n-1)T_f\right) + h_{ij,k}\left(nT_f\right)\right) - \frac{\tau}{T_f}\left(h_{ij,k}\left((n-1)T_f\right) - h_{ij,k}\left(nT_f\right)\right) \end{aligned} \tag{15}$$

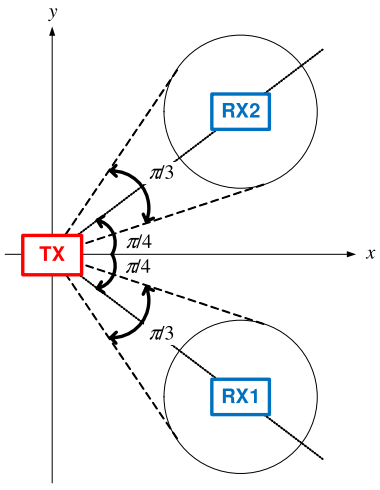

Fig. 2 Positions of TX and RXs (RX1 and RX2). The TX and RXs correspond to the BS and MSs, respectively.

symbols inserted in the packets were transmitted separately in the time domain, and the uplink channels and the effective downlink channels were estimated without interference even in time-varying environments. We assumed that the pilot symbol power for both the uplink channel estimation and the effective downlink channel estimation was equal to that in the duration of data symbol transmission. Each RX determined the minimum mean-squared error (MMSE) weights using its own effective downlink channels. We will explain the propagation environments in the following subsections.

3.1 Jakes' Model

Propagation channels often experience Rayleigh fading in mobile communications, and the Jakes' model can emulate Rayleigh fading environments [18]–[20]. The Jakes' model assumed the TX and RXs were positioned as shown in Fig. 2. The TX and RXs correspond to the BS and MSs that were previously explained. We assumed that there were 13 scatterers uniformly distributed on a ring surrounding each RX, and the angle spread from the TX to each ring of scatterers was equal to $\pi/3$. The number of scatterers, 13, is sufficient for simulating time-correlated Rayleigh fading channels. Also, we do not need to designate the distance between the TX and RXs. The effect of distance attenuation is included in normalized TX power that will be defined in Sect. 3.3. Correlations between channels are related with the angle spread from the TX, and are determined without giving the distance. Arrays with an omnidirectional antenna spacing of 3 cm (half-wavelength at 5 GHz) were along the y-axis, as shown in Fig. 3. Here, we evaluated performance for both cases where there were correlations and no correlations between channels.

Since we assumed the Jakes' model, the 13 scatterers distributed incident waves with an equal amplitude but with randomly different phases. When the channels had correlations, the phases of the waves rotated by the same amount at the same scatterer. Thus, we could achieve correlated

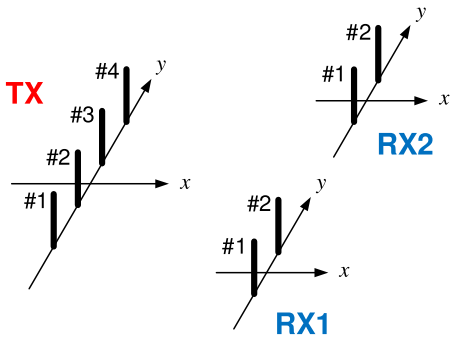

Fig. 3 Configuration of array.

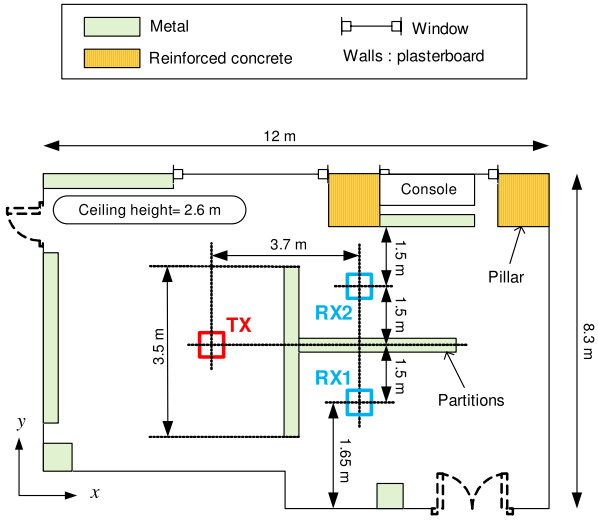

Fig. 4 Measurement site (top view).

Rayleigh fading environments. However, each scatterer in the uncorrelated case independently and randomly rotated the phase of each incident wave. Then, the channels experienced independent and identically distributed Rayleigh fading. The RXs in both cases moved at a constant velocity, and we obtained time-varying Jakes' environments.

3.2 Actual Indoor Environment

The campaign to measure the multi-user MIMO system was carried out in a meeting room in a building of the Graduate School of Information Science and Technology at Hokkaido University, as shown in Fig. 4. The measurements were the same as those done by Bui et al. [6]. The walls of the room were mostly plasterboard. The room also had reinforced concrete pillars, metal doors, and a metal whiteboard. A four-element TX and two two-element RX linear arrays were placed on three tables in the room. The arrays that consisted of omnidirectional collinear antennas were the same as those in Fig. 3. The nominal gain of these antennas on the horizontal plane was about 4 dBi. We examined a non-line-of-sight (NLOS) case where the line-of-sight (LOS) components were blocked by the partitions, as shown in the photograph in Fig. 5. Note that RX2 was be-

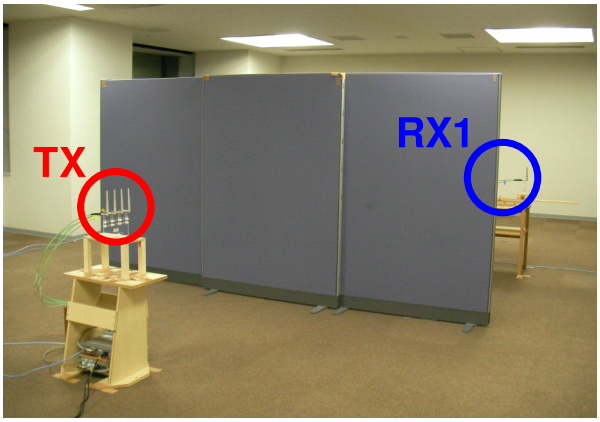

Fig. 5 Measurement environment.

hind the partitions and it has not been shown in the figure.

The measurement band was from 5.15 to 5.40 GHz (bandwidth = 250 MHz), and we obtained 1,601 frequency domain data with 156.25 kHz intervals by using a vector network analyzer. Two stepping motors were used on the RX side to move the two RX arrays along the x-axis during the experiments. Each step of the motors corresponded to 0.088 mm. The channels were measured at intervals of 0.88 mm, and we had a total of 500 spatial measuring points. As a result, $1{,}601 \times 500 = 800{,}500$ MIMO channel response matrices were obtained for each user. Note that the measurement campaign was conducted while there was no one in the room to ensure statistical stationarity of propagation.

3.3 Analyses of Performance

Figures 6 and 7 plot the average packet error rates (PERs) with channel predictions for RX1 versus normalized TX power in the Jakes' model for the former and in the indoor environment for the latter. The solid curves with AR(2), AR(3), and AR(4) indicate the PER using AR-model-based predictions of the orders two, three, and four. Similarly, the dotted curves represent performance using Lagrange extrapolation. Linear, Second, and Third in the figures correspond to linear, second-order, and third-order extrapolations. In addition to PER with the predictions, performance without predictions (Non-Prediction) and that of an ideal case are plotted in the figures. When we did not predict channels, we determined the TX weights and other parameters using the CSI obtained from the latest ACK packet. The ideal case indicated behavior using accurately-predicted channels where not only TX weights but also RX weights were determined based on the correct CSI. The normalized TX power in the Jakes' model is defined as the TX power per MS normalized by the value yielding average E_s/N_0 of 0 dB at the single omni-directional antenna receiver when a signal is transmitted from the single omni-directional antenna. Here, E_s denotes the energy received during a symbol interval and N_0 denotes the thermal noise power spectrum density. The normalized TX power in the indoor environment is the TX power per MS normalized by the power yielding average

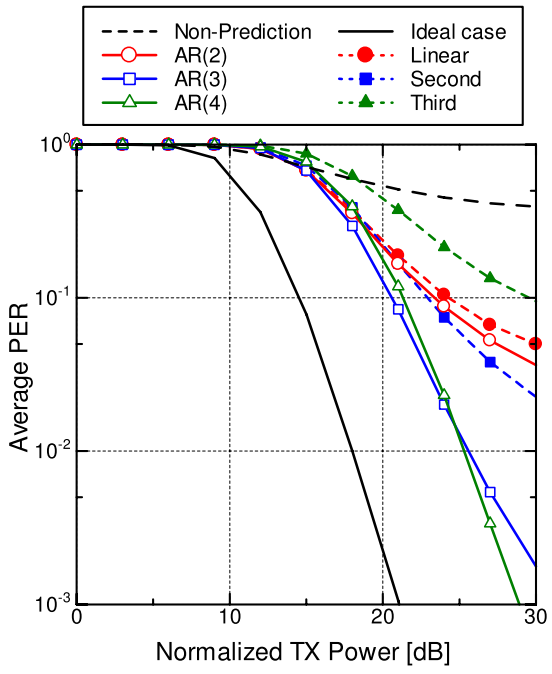

(a) Uncorrelated environment

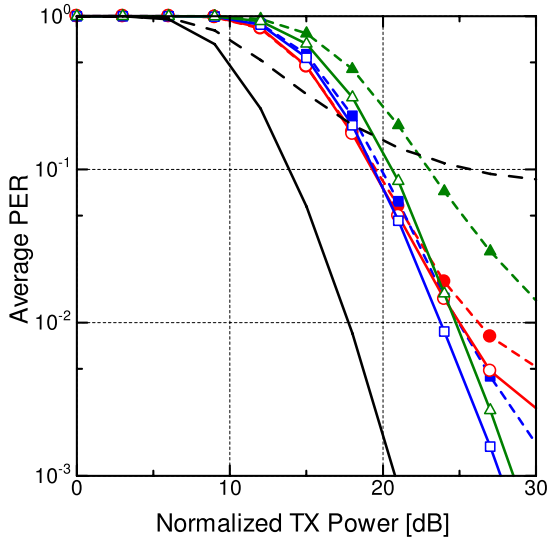

(b) Correlated environment

Fig. 6 Averaged PER of multi-user MIMO systems for RX1 in case of Jakes' model. $N_p = 1$.

E_s/N_0 of 0 dB in single-user single-input single-output LOS measurements in an anechoic chamber. Note that E_s/N_0 is equal to the signal-to-noise ratio (SNR). We assumed the number of pilot symbols (N_p) to estimate channels was one for Figs. 6 and 7(a), and eight for Fig. 7(b). Let us assume that the normalized TX power is $P_{\mathrm{TX,nor}}$ in the Jakes' model. Since the pilot symbols in ACK packets are transmitted separately in the time domain, the average SNR for the uplink channel estimation is equal to $P_{\mathrm{TX,nor}}$. The average SNR for the effective downlink channel estimation is equal to the mean square of each element in $\tilde{\boldsymbol{H}}'_k(t,\tau)$. It should be

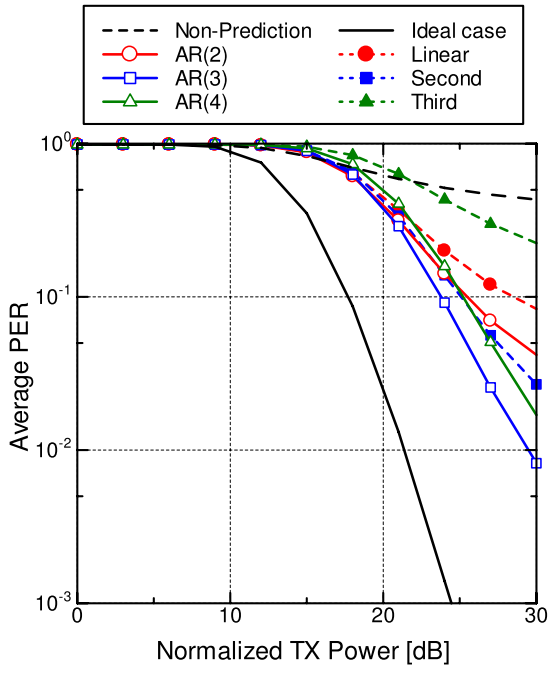

(a) $N_p = 1$

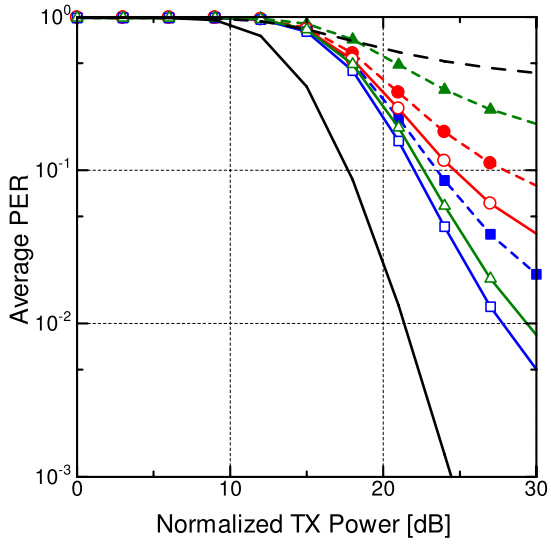

(b) $N_p = 8$

Fig. 7 Averaged PER of multi-user MIMO systems for RX1 in indoor NLOS environment. RX motion along x-axis.

noted that the normalized TX power $P_{\mathrm{TX,nor}}$ is included in the weights as stated in [6]. The average SNR for the channel estimation in the indoor environment can be similarly evaluated. In addition, we assumed that the maximum Doppler frequency was 18.6 Hz at the center frequency, f_c = 5.275 GHz, and the transmission delay, τ, of the downlink packet from the ACK packet was 5 ms.

We can see high error floors in Figs. 6 and 7 when we did not predict the channels. The TX side transmitted at most two streams to each MS. Each MS with two antennas could reduce the IStI because the RX weights were determined based on the MMSE criterion. The RX sides could not, however, reduce the IUI. The TX weights were not optimum because of channel transition during the delay of 5 ms, and they could not suppress the IUI. The error floor for the Jakes' model in the uncorrelated environment (Fig. 6(a)) was higher than that in the correlated environment (Fig. 6(b)) since the channels independently varied in the uncorrelated environment. In contrast, every channel prediction scheme improved performance in higher TX power regions. It can be seen from Figs. 6 and 7 that AR-model-based prediction with the order p of three provides slightly better PER than that with the p of four except where the normalized TX power is higher than 25 dB in the uncorrelated Jakes' environment (Fig. 6(a)). If the estimated channels used for predictions are accurate in the Jakes' model cases, the higher the order is, the better the PER that AR-model-based prediction provides. This is because the autocorrelations were obtained assuming the Jakes' model as given by Eqs. (11) and (12). The estimated channels, however, contained errors since they were obtained with finite pilot symbols. Hence, AR-model-based prediction with a higher order did not necessarily provide better PER even in the Jakes' model cases. It is interesting that predictions assuming the Jakes' model could also achieve significant reductions in PER in the indoor environment (Fig. 7).

Second-order extrapolation achieved the best PER for the Lagrange extrapolation schemes, which is almost the same as that obtained from AR-model-based prediction with the order of four except for the uncorrelated Jakes' model. Third-order extrapolation, on the other hand, had the worst prediction. When we used Lagrange extrapolation, the predicted channels were obtained by calculating a function that had every data point used for prediction. Thus, when the order was higher, the function vibrated greately and degraded the accuracy of prediction.

It can be seen from Fig. 7 that the PER for $N_p = 8$ was better than that for $N_p = 1$. When there were more pilot symbols, channels were estimated more accurately, and this improved performance.

Figures 8 and 9 plot the throughput for RX1 versus the normalized prediction range. The normalized prediction range is a distance (l) where the MSs move during the delay time (τ) normalized by the wavelength (λ) at the center frequency (f_c). The value is written using the maximum Doppler frequency (f_D) as

$$\frac{l}{\lambda} = \frac{v\tau}{\lambda} = \left(\frac{v}{c} f_c\right)\tau = f_D\tau, \tag{16}$$

where v is the velocity of the MSs. The figures plot throughput when we predicted channels at positions with distances of the range from RX1. We changed the normalized prediction range from 0 to 0.186 in the simulations by varying τ from 0 to 10 ms for the fixed value of f_D = 18.6 Hz. Throughput is given by 4 × (1 − Average PER) bps/Hz because the data rate for each MS is 4 bps/Hz. We assumed that the normalized TX power was 25 dB. Note that the throughput for the ideal case is 4 bps/Hz independently of

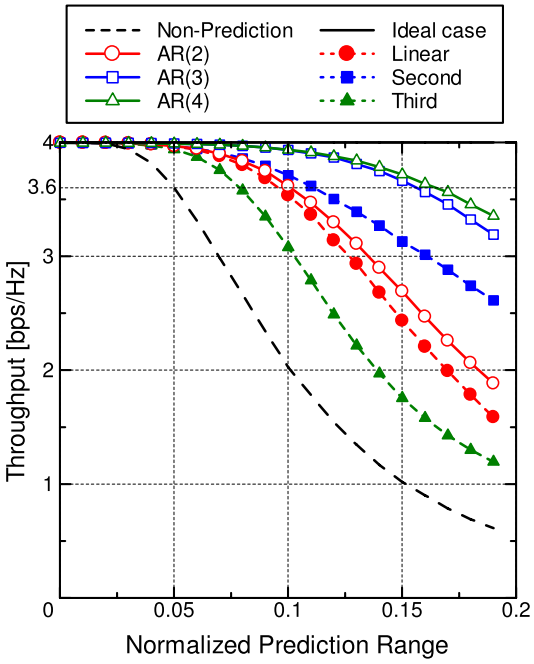

(a) Uncorrelated environment

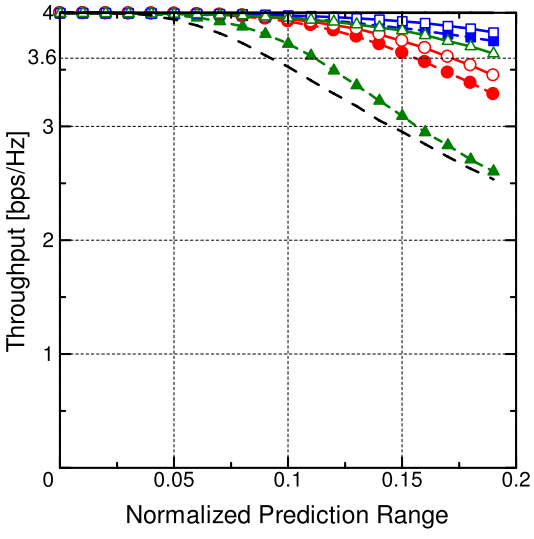

(b) Correlated environment

Fig. 8 Throughput for RX1 versus normalized prediction range at normalized TX power of 25 dB in case of Jakes' model. $N_p = 1$.

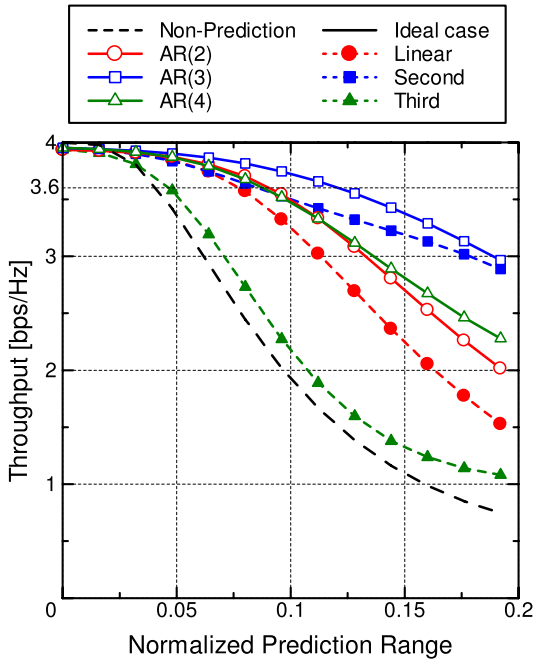

(a) $N_p = 1$

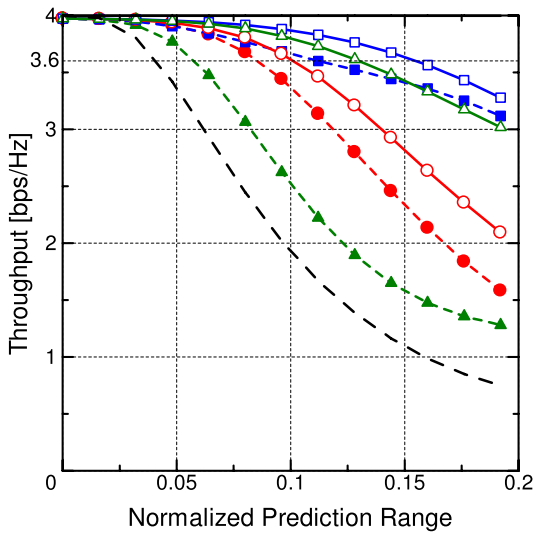

(b) $N_p = 8$

Fig. 9 Throughput for RX1 versus normalized prediction range at normalized TX power of 25 dB in indoor NLOS environment. RX motion is along x-axis.

the normalized prediction range.

As can be seen from these figures, if we did not use the prediction schemes, throughput degraded seriously when the normalized prediction range increased. We considered a normalized prediction range where throughput was maintained above 3.6 bps/Hz to be a 10% degradation value from the ideal case. The normalized prediction range for the uncorrelated Jakes' model (Fig. 8(a)) was wider than 0.15 for the AR-model-based scheme with p of three or four, and was wider than 0.1 for second-order extrapolation. Throughput was higher than 3.6 bps/Hz over the whole range using the three prediction schemes for the correlated Jakes' model (Fig. 8(b)). It should be noted that this performance was obtained using one pilot symbol for each channel ($N_p = 1$). However, throughput in the indoor environment for $N_p = 1$ (Fig. 9(a)) was worse than that in the Jakes' model cases. Performance could, however, be improved by using more pilot symbols. It can be seen from Fig. 9(b) that the throughput for $N_p = 8$ is above 3.6 bps/Hz in normalized prediction ranges wider than 0.1 if we use second-order extrapolation or AR-model-based prediction with p of three or four.

4. Conclusion

We investigated what effects channel predictions using an AR-model-based scheme and Lagrange extrapolation would have on a multi-user MIMO system. These considerations were done in the presence of channel estimation error. We found that every prediction scheme could improve performance. The effect of prediction differed depending on the order of the AR model in the AR-model-based predictor. Lagrange extrapolation could provide performance comparable to that of AR-model-based prediction without statistical quantities that were not necessarily easy to estimate. We found that second-order extrapolation could predict channels in normalized prediction ranges over 0.1 within a throughput degradation of 10%. Since Lagrange extrapolation is easy to implement, prediction schemes using it can play important roles in multi-user MIMO systems.

References

[1] Q.H. Spencer, C.B. Peel, and A.L. Swindlehurst, "An introduction to the multi-user MIMO downlink," IEEE Commun. Mag., vol.42, no.3, pp.60–67, Oct. 2004.
[2] D. Gesbert, M. Kountouris, R. Heath, C.-B. Chae, and T. Salzer, "Shifting the MIMO paradigm," IEEE Signal Process. Mag., vol.24, no.5, pp.36–46, Sept. 2007.
[3] Q.H. Spencer, A.L. Swindlehurst, and M. Haadt, "Zero-forcing methods for downlink spatial multiplexing in multiuser MIMO channels," IEEE Trans. Signal Process., vol.52, no.2, pp.461–471, Feb. 2004.
[4] R.L.U. Choi and R.D. Murch, "A transmit preprocessing technique for multiuser MIMO systems using a decomposition approach," IEEE Trans. Wireless Commun., vol.3, no.1, pp.20–24, Jan. 2004.
[5] K. Miyashita, T. Nishimura, T. Ohgane, Y. Ogawa, Y. Takatori, and K. Cho, "High data-rate transmission with eigenbeam-space division multiplexing (E-SDM) in a MIMO channel," Proc. IEEE VTC 2002 Fall, vol.3, pp.1302–1306, Sept. 2002.
[6] H.P. Bui, Y. Ogawa, T. Nishimura, and T. Ohgane, "Performance evaluation of a multi-user MIMO system with prediction of time-varying indoor channels," IEEE Trans. Antennas Propag., vol.61, no.1, pp.371–379, Jan. 2013.
[7] A. Duel-Hallen, "Fading channel prediction for mobile radio adaptive transmission systems," Proc. IEEE, vol.95, no.12, pp.2299–2313, Dec. 2007.
[8] J.B. Andersen, J. Jensen, S.H. Jensen, and F. Frederiksen, "Prediction of future fading based on past measurements," IEEE VTC 1999 Fall, vol.1, pp.151–155, Sept. 1999.
[9] T. Eyceoz, A. Duel-Hallen, and H. Hallen, "Deterministic channel modeling and long range prediction of fast fading mobile radio channels," IEEE Commun. Lett., vol.2, pp.254–256, Sept. 1998.
[10] N. Palleit and T. Weber, "Channel prediction in multiple antenna systems," 2012 International ITG Workshop on Smart Antennas (WSA), pp.1–7, March 2012.
[11] T. Ekman, Prediction of mobile radio channel — Modeling and design, Ph.D. dissertation, Uppsala University, Uppsala, Sweden, 2002.
[12] L. Dong, G. Xu, and H. Ling, "Prediction of fast fading mobile radio channels in wideband communication systems," Proc. IEEE GLOBECOM, vol.6, pp.3287–3291, Nov. 2001.
[13] K.E. Baddour and N.C. Beaulieu, "Autoregressive modeling for fading channel simulation," IEEE Trans. Wireless Commun., vol.4, pp.1650–1662, July 2005.
[14] K. Yamaguchi, H.P. Bui, Y. Ogawa, T. Nishimura, and T. Ohgane, "Considerations on a multi-user MIMO system using channel prediction based on an AR model," Proc. IEEE AP-S/URSI 2013, July 2013.
[15] Y. Ogawa, K. Yamaguchi, H.P. Bui, T. Nishimura, and T. Ohgane, "Behavior of a multi-user MIMO system in time-varying environments," IEICE Trans. Commun., vol.E96-B, no.10, pp.2364–2371, Oct. 2013.
[16] R.W. Schafer and L. Rabiner, "A digital signal processing approach to interpolation," Proc. IEEE, vol.61, pp.692–702, June 1973.
[17] H. Matsui and A. Hirose, "Nonlinear prediction of frequency-domain channel parameters for channel prediction in fading and fast Doppler-shift change environment," Proc. ISAP2012, Oct./Nov. 2012.
[18] W.C. Jakes, Microwave Mobile Communications, pp.13–17, Wiley-IEEE Press, Piscataway, NJ, 1994.
[19] P. Dent, G.E. Bottomley, and T. Croft, "Jakes fading model revisited," Electron. Lett., vol.29, no.13, pp.1162–1163, June 1993.
[20] H. Iwai, Radio Propagation in Mobile Communications, — Fundamental Knowledge for Simulation Analysis of Wireless Communications, pp.88–94, Corona Publishing, Tokyo, 2012. (in Japanese)

Kanako Yamaguchi received her B.E. from Hokkaido University in Sapporo, Japan, in 2012. Her interests are in MIMO systems and mobile communications.

Huu Phu Bui received his B.S. in electronics engineering from Danang University in 1997 and his M.S. in electronics engineering from Hochiminh City University in 2002, both in Vietnam. He received his Ph.D. in information science and technology from Hokkaido University, Japan in 2007. From 1997 to 200, he was with the Radio Frequency Directorate of the Ministry of Information and Communications, Vietnam. From 2008 to 2011, he was with Hochiminh City University of Science, Vietnam. He is currently a Vice Director of the Vietnam National Key Laboratory of Digital Control and System Engineering at the Hochiminh City University of Technology. From 2007 to 2009, he was a postdoctoral researcher at Hokkaido University, Japan. His research interests are in channel prediction and signal processing for MIMO systems. He received the IEEE VTS Japan Chapter Young Researcher's Encouragement Award in 2006.

Yasutaka Ogawa received his B.E., M.E., and Ph.D. from Hokkaido University, Sapporo, Japan, in 1973, 1975, and 1978. Since 1979, he has been with Hokkaido University, where he is currently a full Professor at the Graduate School of Information Science and Technology. In 1992–1993, he was with the Electro Science Laboratory of Ohio State University, U.S.A., as a Visiting Scholar, on leave from Hokkaido University. His interests are in adaptive antennas, mobile communications, super-resolution techniques, and MIMO systems. He received the Yasujiro Niwa outstanding paper award in 1978, the Young Researchers' Award of IEICE Japan in 1982, the Best Paper Award from IEICE Japan in 2007, and the Best Magazine Paper Award in 2011 from the IEICE Communications Society. He is a Fellow of the IEEE.

Toshihiko Nishimura received his B.S. in physics in 1992, his M.S. in physics in 1994, and his Ph.D. in electronics engineering in 1997 all from Hokkaido University, Sapporo, Japan. He joined the Graduate School of Engineering (now reorganized as the Graduate School of Information Science and Technology) at Hokkaido University in 1998, where he is currently an Assistant Professor of the Graduate School of Information Science and Technology. His current research interests are in MIMO systems using smart antenna techniques. He received the Young Researchers' Award of IEICE Japan in 2000, the Best Paper Award from IEICE Japan in 2007, and the Best Magazine Paper Award in 2011 from the IEICE Communications Society. He is a member of the IEEE.

Takeo Ohgane received his B.E., M.E., and Ph.D. in electronics engineering from Hokkaido University, Sapporo, Japan, in 1984, 1986, and 1994. He was with the Communications Research Laboratory of the Ministry of Posts and Telecommunications from 1986 to 1992. He was on assignment at the ATR Optical and Radio Communications Research Laboratory from 1992 to 1995. Since 1995, he has been with Hokkaido University, where he is an Associate Professor. He was at the Centre for Communications Research of the University of Bristol, U.K., as a Visiting Fellow in 2005–2006. His interests are in MIMO signal processing for wireless communications. He received the Young Researchers' Award of IEICE Japan in 1990, the IEEE AP-S Tokyo Chapter Young Engineer Award in 1993, the Best Paper Award from IEICE Japan in 2007, and the Best Magazine Paper Award in 2011 from the IEICE Communications Society. He is a member of the IEEE.